ASME-ATI-UIT Conference on Thermal and Environmental Issues in Energy Systems
16 - 19 May, 2010, Sorrento, Italy

MODELLING OF MOLECULAR ORIENTATION AND CRYSTALLIZATION IN THE MANUFACTURE OF SEMI–CRYSTALLINE COMPOUND FIBRES

Francisco J. Blanco–Rodríguez* and J.I. Ramos**

*Room 2.140.D, Escuela de Ingenierías, Doctor Ortiz Ramos, s/n, Universidad de Málaga, 29071 Málaga, Spain, E-mail: fjblanco@lcc.uma.es, Phone:(+34) 951952522
**Room 2.139.D, Escuela de Ingenierías, Doctor Ortiz Ramos, s/n, Universidad de Málaga, 29071 Málaga, Spain, E-mail: jirs@lcc.uma.es, Phone:(+34) 951952387

ABSTRACT

In this paper, we present a two–dimensional model of the fluid dynamics, heat transfer, molecular orientation and crystallization processes that occur in the manufacture of semi–crystalline compound fibres by melt–spinning processes. The model employs a Newtonian rheology, includes the effects of both temperature and flow–induced crystallization, and accounts for the effects of the molecular orientation on both the stress tensor and the crystallization through a Doi–Edwards formulation. It is shown that, even at moderate low Biot numbers, the temperature across the compound fibre is not uniform owing to the heat loss and thermal boundary layer at the cladding's outer interface. However, the cross–sectional averaged temperature exhibits the same qualitative trends as those of an asymptotic one–dimensional model which is valid for slender fibres at low Reynolds and Biot numbers.

INTRODUCTION

In the fabrication of bi–component textile, electrically conducting, optical or reinforced fibres, two polymers are co–extruded through a small hole in a plate into ambient air to form a compound fibre. These fibres consist of a core and a cladding of, in general, different characteristics that are either extruded trough an annular nozzle or are produced by heating a perform to above its melting temperature and then extruding the resulting melt trough an annular nozzle. In some of these fibres, the cladding material either protects the core, serves as a waveguide in signal transmission or is a more costly material than the core with more desirable surface properties. Depending on the extrusion conditions and the rheology of the core and cladding, the compound fibre may swell after exiting the nozzle.

The properties of plastic products manufactured by heating the polymer to above its melting temperature and then deforming the melt while simultaneously cooling it, depend on the processing conditions to which the polymer is subject during its manufacture. Furthermore, depending on the molecular structure and processing conditions, the final product can be in either an amorphous or semi–crystalline state. Polymers that are unable to crystallize on cooling below their glass transition temperature, form amorphous solids, and, if these solids are formed by deforming the polymer while cooling it through the glass transition temperature, they can exhibit strong anisotropy.

Previous studies of bi–component fibres have been mainly concerned with one–dimensional models of amorphous, slender fibres at low Reynolds numbers based on either simplified models, Taylor's series expansion or an asymptotic analysis of the full governing equations that uses the slenderness ratio as the small perturbation parameter. In addition, these studies have been mainly concerned with isothermal flows [1; 2; 3; 4; 5]. Non–isothermal studies of bicomponent fibres include that of Kikutani et al. [6] who modelled the high–speed melt spinning of bicomponent fibres consisting of poly (ethylene terephthalate) (PET) in the core and polypropelene (PP) in the cladding by means of simple, one–dimensional equations of mass, linear momentum and energy conservation, and included both Newtonian and upper–convected Maxwell rheologies and drag on the fibre.

An asymptotic one–dimensional model of semi–crystalline, bi–component fibres that includes molecular orientation and crystallization but does not include the latent heat of crystallization was developed by the one of the authors [7]. Such a model is governed by one–dimensional partial differential equations for the leading–order (in the slenderness ratio) geometry, axial velocity component and temperature that were derived from the conservation equations of mass, linear momentum and energy under the assumptions that the fibre is slender and the Reynolds and Biot numbers are small. The effects of the molecular orientation and crystallization were added to this model by considering two transport equations for these two quantities. The molecular orientation model was based on Doi's theory for liquid crystalline polymers, while the crystallization kinetics used Avrami–Kolmogorov's theory [8; 9] with Ziabicki's model [10] for the coupling between the crystallinity and the polymer orientation, and Kikutani's empirical law [11; 12] was employed to relate the elongational viscosity of the melt to the degree of crystallinity. In this paper, we present a two–dimensional model of semi–crystalline bi–component fibre spinning processes that uses a modified Newtonian rheology, accounts for the degrees of molecular orientation and crystallization, and allows to determine the radial variations of these quantities across the compound fibre.

MATHEMATICAL FORMULATION

We consider an axisymmetric, bi–component or compound liquid jet such as the one shown schematically in Fig. 1, consis-

ting of two immiscible, incompressible (constant density) polymers. The inner (subscript 1) and outer (subscript 2) jets correspond to $0 \le r \le R_1(t,x) \equiv R(t,x)$ and $R_1(t,x) \le r \le R_2(t,x)$, respectively. In order to model the fluid dynamics, heat transfer, molecular orientation and crystallization processes that occur in the manufacture of semi–crystalline compound fibres, we have assumed that the rheology of the core and cladding is Newtonian. Furthermore, we shall be concerned with the processes that occur beyond the swelling section ($x = 0$) where the external radius of the fibre is a decreasing function of the axial distance and where cooling due to forcing of the surrounding media and radiation cause a radial temperature distribution across each section of the fibre which, in turn, results in a radial variation of the dynamic viscosity of the materials.

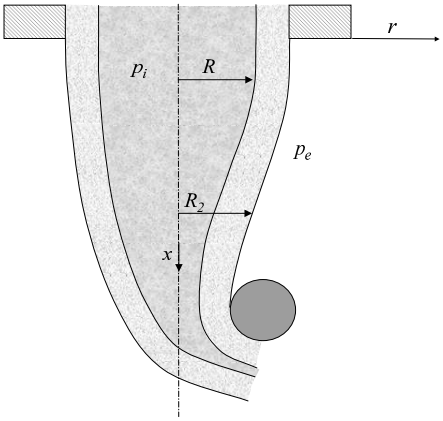

Figure 1. Schematic of a compound fibre.

The fluid dynamics of bicomponent fibres are governed by the two–dimensional conservation equations of mass (1), linear momentum (2) and energy (3),

$$\nabla \cdot \mathbf{v}_i = 0 \qquad i = 1, 2, \tag{1}$$

$$\rho_i \left(\frac{\partial \mathbf{v}_i}{\partial t} + \mathbf{v}_i \cdot \nabla \mathbf{v}_i \right) = -\nabla p_i + \nabla \cdot \tau_i + \rho_i \cdot \mathbf{f}_i^m \qquad i = 1, 2, \tag{2}$$

$$\rho_i C_i \left(\frac{\partial T_i}{\partial t} + \mathbf{v}_i \cdot \nabla T_i \right) = k_i \Delta T_i \qquad i = 1, 2, \tag{3}$$

where $\mathbf{v} = u\,\hat{\mathbf{e}}_\mathbf{x} + v\,\hat{\mathbf{e}}_\mathbf{r}$ and $\mathbf{f}^m = g\,\hat{\mathbf{e}}_\mathbf{x}$.

In the model presented here, we shall assume that the density, specific heat, thermal conductivity and surface tension are constant, and that the gases surrounding the outer jet are dynamically passive. The latter assumption can be justified due to the small density and dynamic viscosity of gases compared with those of liquids. In addition, it is assumed that the dynamic viscosity of the two components of the fibre depends on a linearized Arrhenius fashion on the temperature, and can be written as

$$\mu_i(T_i) = D_i \exp\left(H_i\left((T_m)_i - T_i\right)\right) \qquad i = 1, 2, \tag{4}$$

which indicates that the dynamic viscosity increases exponentially with the temperature for $T < T_m$.

Polymer molecules that form liquid–crystalline phases in solution generally have rigid backbones and consequently have rod–like or disk–like shapes. In this paper, we model the solution of rod–like polymers as an ensemble of rigid dumbbells suspended in a Newtonian solvent. In such a solution, the deviatoric stress tensor is assumed to be

$$\tau = \mu_{eff}(\nabla \mathbf{v} + (\nabla \mathbf{v})^T) + \tau_\mathbf{p}, \qquad i = 1, 2, \tag{5}$$

where

$$\tau_\mathbf{p} = 3ck_BT(-\lambda F(\mathbf{S})/\phi + 2\lambda((\nabla \mathbf{v})^T : \mathbf{S})(\mathbf{S} + \mathbf{I}/3)), \tag{6}$$

and $\mathbf{I}$ is the identity or unit tensor and λ follows, as the dynamic viscosity, an Arrhenius fashion,

$$\lambda_i = \lambda_{i,0} \exp\left(\omega_i\left((T_m)_i - T_i\right)\right) \qquad i = 1, 2. \tag{7}$$

Taking moments of the probability density function for the molecular orientation and modelling the fourth–order moments in terms of second–order ones, result in the following partial differential equation for the molecular orientation tensor which depends on the strain rate and the relaxation of the molecular chains,

$$\frac{\partial \mathbf{S}}{\partial t} + \mathbf{v} \cdot \nabla \mathbf{S} = (\nabla \mathbf{v})^T \cdot \mathbf{S} + \mathbf{S} \cdot \nabla \mathbf{v} + F(\mathbf{S}) + G(\nabla \mathbf{v}, \mathbf{S}), \tag{8}$$

where $\mathbf{S}$ is traceless,

$$F(\mathbf{S}) = -\frac{\phi}{\lambda}((1 - N/3)\mathbf{S} - N(\mathbf{S} \cdot \mathbf{S}) + N(\mathbf{S} : \mathbf{S})(\mathbf{S} + \mathbf{I}/3)), \tag{9}$$

$$G(\nabla \mathbf{v}, \mathbf{S}) = (\nabla \mathbf{v} + (\nabla \mathbf{v})^T)/3 - 2((\nabla \mathbf{v})^T : \mathbf{S})(\mathbf{S} + \mathbf{I}/3), \tag{10}$$

and N is a dimensionless measure of the polymer number density (c) and is directly proportional to the excluded volume between two rigid rods where each rod represents a polymer molecule, $0 \le \phi \le 1$ is a nondimensional parameter related to the friction tensor ($\phi = 1$ corresponds to an isotropic friction tensor and smaller values of ϕ corresponds to increasing the ratio of the resistance encountered perpendicularly to the dumbbell to that encounter parallel to the axis of the dumbbell). Doi's equation for the molecular orientation tensor corresponds to changing ϕ/λ for $6D_R$ where D_R is an averaged rotational diffusion coefficient, and $\mathbf{S} = <\mathbf{uu} - \mathbf{I}/3>$ where $\mathbf{u}$ denotes the molecular orientation vector. The molecular orientation parameter $\mathcal{S}$ is defined by

$$\mathcal{S} = \sqrt{\frac{3}{2}(\mathbf{S} : \mathbf{S})}. \tag{11}$$

In order to account for the effects of both amorphous and crystalline phases, we have assumed that the semi–crystalline materials that compose the core and cladding behave as single–phase

fluids where the degree of crystallization ($\mathcal{X}$) has been modelled by means of Ziabicki's model [12], i.e.,

$$\frac{\partial \mathcal{X}_i}{\partial t} + \mathbf{v}\cdot\nabla\mathcal{X}_i = k_{Ai}(\mathcal{S})(\mathcal{X}_{\infty,i} - \mathcal{X}_i) \qquad i = 1, 2, \tag{12}$$

where $k_{Ai}(\mathcal{S}) = k_{Ai}(0)\exp(a_{2i}\mathcal{S}_i^2)$ is the linearized crystal growth rate. The effective viscosity that appears in Eq. (5) can be written as

$$\mu_{eff,i} = \mu_i(T_i)\exp\left(\beta_i\left(\frac{\mathcal{X}_i}{\mathcal{X}_{\infty,i}}\right)^{n_i}\right) \qquad i = 1, 2, \tag{13}$$

where β and n are material–dependent, e.g., $\beta_i = 4.605$ and $n_i = 12$ for nylon–66, $\beta_i = 4$ and $n_i = 2$ for PET, and the effects of crystallization on the effective dynamic viscosity have been assumed to be multiplicative. Equation (13) indicates that, in addition to the contribution of the molecular orientation to the deviatoric stress tensor (cf. Eq. (5)), the degree of crystallization affects the effective viscosity and, therefore, the Newtonian stress tensor (cf. Eq. (5)).

In this paper, it is assumed that the molecular orientation tensor is symmetric and, therefore, has only six components. However, since this tensor is traceless ($S_{rr} + S_{\theta\theta} + S_{xx} = 0$), one of the components in the main diagonal can be related to the other two and, therefore, it only has five different components. Moreover, for slender fibres, it is an easy exercise using perturbation methods based on the slenderness ratio (ε) that S_{rx} must be $O(\varepsilon)$, and, therefore, this component does not appear in the (one–dimensional) equations at leading–order in the slenderness ratio. Furthermore, by assuming that $S_{\theta x} = S_{r\theta} = 0$ where θ denotes the azimuthal coordinate, the molecular orientation tensor becomes diagonal with only two independent components. If, in addition, $S_{rr} = S_{\theta\theta} = -S_{xx}/2 = -\mathcal{S}/3$, the resulting tensor is proportional to the leading–order velocity tensor for slender fibres and the stress tensor τ adopts a expression like

$$\tau = \hat{\mu}_{eff}(\nabla\mathbf{v} + (\nabla\mathbf{v})^T), \qquad i = 1, 2, \tag{14}$$

where

$$\hat{\mu}_{eff,i} = \mu_i(T_i)\exp\left(\beta_i\left(\frac{\mathcal{X}_i}{\mathcal{X}_{\infty,i}}\right)^{n_i}\right) + \frac{2}{3}\alpha_i\lambda_i T_i \mathcal{S}_i^2. \tag{15}$$

Equations (8) and (12) together with the Navier–Stokes equations (1–3) and Eq. (13), govern the fluid dynamics of semi–crystalline compound fibres and are subject to specified conditions at the nozzle exit, $x = 0$, downstream or take–up location, $x = L$, initial conditions and symmetry boundary conditions at centerline $r = 0$. In addition, at the to–be–determined core–cladding, $r = R_1(t,x)$, and cladding–surrounding, $r = R_2(t,x)$, interfaces where these are assumed to be material surfaces, kinematic and dynamic boundary conditions that specify the continuity of axial and radial velocity components and tangential stresses, and the balance of the normal stress difference with surface tension, must be applied. Moreover, at $r = R_1$, there is continuity of temperatures and heat flux, while, at $r = R_2$, the heat flux from conduction in the cladding was assumed to be equal to $h(T(t,R_2,x) - T_\infty)$ and the film heat transfer coefficient h could depend on the local Reynolds and Prandtl numbers [13].

NUMERICAL METHOD

For slender fibres, $\varepsilon = R_0/L << 1$, it is convenient nondimensionalize the variables r, x, t, u, v, p, T, ρ, C, μ and k with respect to R_0, L, $t_0 = L/u_0$, u_0, $v_0 = \varepsilon u_0$, $p_0 = \mu_0 u_0/L$, T_0, ρ_0, C_0, μ_0 and k_0 respectively, where R_0 is the die exit radius and L is the distance between the die exit and take–up location. With this nondimensionalization, the dimensionless parameters governing the problem are the Reynolds, $Re = \frac{\rho_0 u_0 R_0}{\mu_0}$, Froude, $Fr = \frac{u_0^2}{g R_0}$, capillarity, $Ca = \frac{\mu_0 u_0}{\sigma_2}$, Peclet, $Pe = \left(\frac{\rho_0 C_0}{k_0}\right) u_0 R_0$ and Biot, $Bi = \frac{h R_0}{k_2}$, numbers.

For steady–state slender fibres at low Reynolds and Biot numbers, it can be easily shown by means of perturbation methods based on the slenderness ratio that the leading–order axial velocity component is only a function of $\hat{x}$ and the dimensionless volumetric flow rates for the core and cladding are

$$Q_1 = \frac{\mathcal{R}_1^2(\hat{x})}{2}\,\mathcal{U}(\hat{x}), \qquad Q_2 = \frac{\mathcal{R}_2^2(\hat{x}) - \mathcal{R}_1^2(\hat{x})}{2}\,\mathcal{U}(\hat{x}), \tag{16}$$

where $\mathcal{R}_i = \frac{R_i}{R_0}$ and $\mathcal{U} = \frac{u_1(\hat{x})}{u_0} = \frac{u_2(\hat{x})}{u_0}$.

In this paper, we are only concerned with steady state conditions and the numerical solution of the equations governing the two–dimensional free–surface model for semi–crystalline compound fibres presented in the last section was obtained as follows. First, the following transformation $(r,x) \to (\xi,\eta)$ for the inner and outer jets, where $\xi = \frac{\hat{r}}{\mathcal{R}_2(\hat{x})}$ and $\eta = \hat{x}$, was employed to map the curvilinear geometries of the inner and outer fibres into rectangles, i.e., $[0, \mathcal{R}_1(\hat{x})] \to [0, \sqrt{Q_1/Q}]$ and $[\mathcal{R}_1(\hat{x}), \mathcal{R}_2(\hat{x})] \to [\sqrt{Q_1/Q}, 1]$, respectively, where $Q = Q_1 + Q_2$ denotes the nondimensional volumetric flow rate of the compound jet. Under these conditions, the axial momentum equation is one–dimensional and of the advection–diffusion type, whereas the continuity equations for the core and cladding (16) provide $\mathcal{R}_1(\hat{x})$ and $\mathcal{R}_2(\hat{x})$. The equation for the molecular orientation tensor and the degree of crystallization are hyperbolic and can be solved by means of an implicit method, whereas the (two–dimensional) energy equation is of the advection–diffusion type and was solved iteratively in the radial direction in grids consisting of 1001 and 301 points in the axial and radial directions (101 for the core and 201 for the cladding), respectively, until the L_2 norm of the differences between the solutions in two successive iterations was less than or equal to 10^{-8}.

NUMERICAL RESULTS

Some sample two–dimensional results of the axisymmetric melt spinning model for semi–crystalline compound fibres described above are presented here and correspond to the same thermal conductivities and pre–exponential factors and activation energies of the dynamic viscosity for the core and cladding, no surface tension, a constant film–heat transfer coefficient that corresponds to Biot numbers equal to one and five, and unity Reynolds and Froude numbers. By imposing $\mathcal{R}_1(0) = 1$ and $Q_1 = 0.5$ (we have used the same nondimensional volumetric flow for the core and the cladding, $Q_1 = Q_2$), the nondimensional axial velocity (cf. Eq. (16)) at the die exit is unity. In the cases considered here, the draw ratio, D_r, the relation between the axial velocity at the take–up location and that at the nozzle exit is 100. The relevant simulation parameters are summarized in Table 1 where $Pe_i = Pe\left(\frac{\rho_i C_i}{k_i}\right)$.

Table 1. Simulation parameters.

Case	H_1	H_2	Pe_1	Pe_2	Bi	$\frac{k_2}{k_1}$	$\frac{D_2}{D_1}$	ϕ_i	$1/Ca$
1	30	30	1	5	5	1	1	0.5	0
2	30	30	1	5	1	1	1	0.5	0

The other parameters of the problem have been selected as $N_i = 4$, $\alpha_i = 5$, $a_{21} = 10$, $a_{22} = 5$, $\lambda_{i,0} = 1$, $\omega_i = 0$, $\mathcal{X}_{\infty,i} = 0.8$, $n_i = 12$, $\beta_i = 4$, $\frac{\sigma_1}{\sigma_2} = 1$, $k_{A1}(0) = k_{A2}(0) = 0.005$, and $T_\infty = 0$.

The following parabolic profile for the temperature of the compound fibre at the die exit ($\eta = 0$) was imposed

$$\hat{T}(\xi,0) = \begin{cases} 1+\Delta_T\left(1-\left(\frac{\xi}{\xi_i}\right)^2\right) & 0 \le \xi \le \xi_i \\ 1-\Delta_T\left(\frac{\hat{k}_1}{k_2}\right)\left(\left(\frac{\xi}{\xi_i}\right)^2-1\right) & \xi_i \le \xi \le 1 \end{cases} \tag{17}$$

where $\xi_i = \sqrt{\frac{Q_1}{Q}}$ and $\Delta_T < \left(\frac{\hat{k}_2}{k_1}\right)\left(\frac{Q_1}{Q_2}\right)$ because $\hat{T}(1,0) > 0$, and the molecular orientation parameter S

$$S(\xi,0) = \begin{cases} S_{10}-\Delta_{S1}\left(1-2\left(\frac{\xi}{\xi_i}\right)^2\right) & 0 \le \xi \le \xi_i \\ S_{20}+\Delta_{S2}\left(1-\frac{2}{\left(\frac{1-\xi_i}{2}\right)^2}(\xi-1)(\xi_i-\xi)\right) & \xi_i \le \xi \le 1 \end{cases} \tag{18}$$

where $\Delta_{Si} < \min(S_{i0}, 1-S_{i0})$ for $i = 1,2$. For the results presented in the next section, $\Delta_T = 0.1$ and $(S_{10}, \Delta_{S1}) = (0.25, 0.10)$ and $(S_{20}, \Delta_{S2}) = (0.50, 0.20)$ have been used.

Two–dimensional model numerical results

Figure 2 illustrates that the axial velocity component (a) is uniform across the compound fibre, while the radial one (b) is directed towards the symmetry axis ($\hat{v} = -\frac{\hat{r}}{2}\frac{\partial \mathcal{U}}{\partial \hat{x}}$, cf. Eq. (1)) at a rate which first increases and then decreases along the fibre, before it reaches a nil value upon crystallization.

Figure 3 exhibits the thermal boundary layer which is formed at the cladding–surrounding medium interface for both simulation cases and shows that the temperature of the core is nearly uniform in the radial direction up to an axial distance equal to about one half and one quarter of the length of the fibre for cases 1 and 2, respectively. Figure 3 also shows that the contraction of the compound fibre increases as the Biot number is increased on account of the increase in the dynamic viscosity due to the increase in the heat transfer at this number is increased and the no radial dependence of the axial velocity. Figure 3 also indicates that the thermal penetration depth is roughly proportional to the Biot number.

Figure 4 shows that, for the conditions considered here, the degree of crystallization is mainly a function of the temperature, i.e., it increases as the temperature decreases, in accord with the thermal formulation corresponding to the Avrami–Kolmogorov crystallization formalism, and depends very little on the degree of molecular orientation and the flow strain. This is due to the rapid molecular orientation observed in Fig. 5 and the large increase in dynamic viscosity of both the core and the cladding (cf. Fig. 5). Figure 5 also shows that the effective dynamic viscosity of the fibre increases by almost five orders of magnitude from the swelling section to the take–up location.

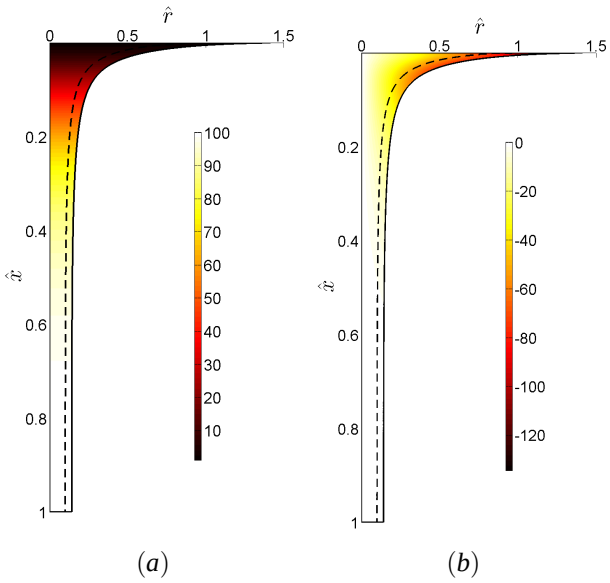

Figure 2. Two–dimensional nondimensional axial velocity (a) and radial velocity (b) for Case 1.

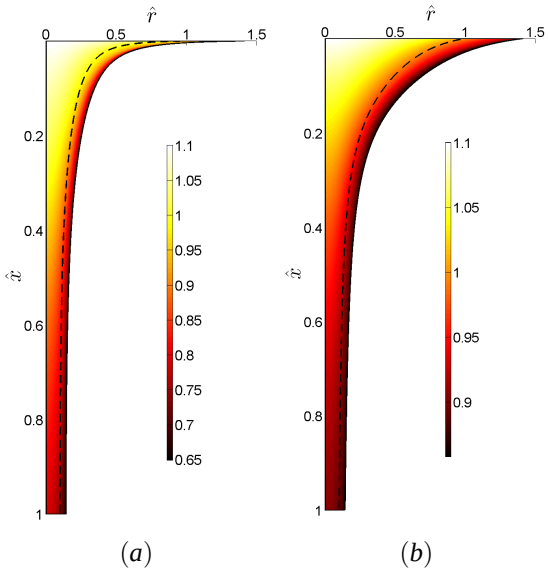

Figure 3. Nondimensional thermal fields for (a) Case 1 ($Bi = 5$) and (b) Case 2 ($Bi = 1$).

Comparison with the one–dimensional model

In this subsection, we compare the results obtained with the two–dimensional model presented here with those of the asymptotic one–dimensional model [5] that uses the slenderness ratio ($\varepsilon = R_0/L$) as a perturbation parameter and results in a set of one–dimensional equations for the fibre's radii, axial velocity component and temperature; however, the temperature of the one–dimensional model employed here is the cross–sectionally

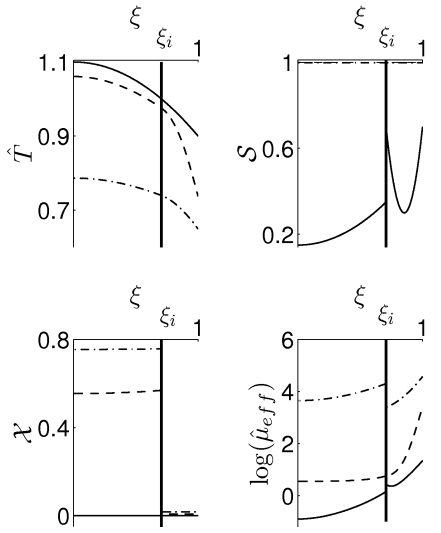

Figure 4. (From left to right, from top to bottom) Temperature, molecular orientation parameter, degree of crystallization and (decimal logarithm of) dynamic viscosity at the "die exit" ($\hat{x} = 0$) (–), $\hat{x} = 0.1$ (– –) and take–up point, $\hat{x} = 1$ (– · –) for Case 1.

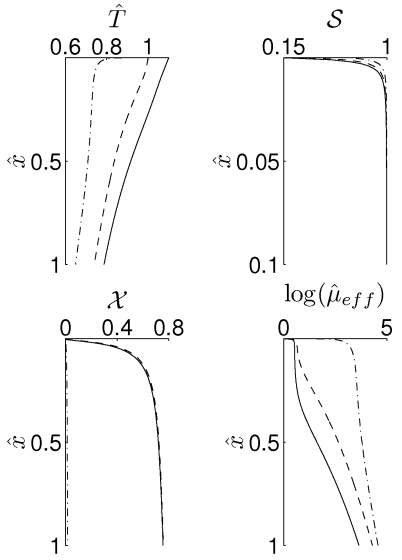

Figure 5. (From left to right, from top to bottom) Temperature, molecular orientation parameter, degree of crystallization and (decimal logarithm of) dynamic viscosity at the axis ($\hat{r} = 0$) (–), core–cladding internal interface ($\hat{r} = \mathcal{R}_1^-$) (– –) and air–cladding interface ($\hat{r} = \mathcal{R}_2$) (–· –) for Case 1.

average of that of the two–dimensional model. Since these averaged temperature includes the radial variations of the thermal fields at, especially, the inner–outer fibre and outer fibre–surrounding medium interfaces and the formulation of the two–dimensional model is also valid for large Biot numbers, what is referred to here as one–dimensional model is not the same as the asymptotic model [5] which requires small Reynolds and Biot numbers and yields, at first–order in the slenderness ratio, a uniform temperature field at each axial location along the compound fibre.

As indicated above, the two–dimensional model uses one–dimensional equations for the geometry and axial velocity component but solves the 2D advection–diffusion equation for the temperature and the hyperbolic equations for the molecular orientation and degree of crystallization. This 2D model shows that the temperature of the core is higher than that of the cladding because of heat losses. Figure 6 shows that the axial velocity exhibits a sigmoid shape characterized by a positive slope that levels off at about a non–dimensional distance from the nozzle equal to 0.5. From Fig. 6, it can be concluded that the 2D model yields a cross–sectionally averaged temperature that exhibits the same qualitative features as that of the one–dimensional model. However, the 1D model is not able to predict accurately the temperature near the symmetry axis and near the cladding–surrounding medium. It must be noted that despite these temperature differences between the 1D and 2D models near the symmetry axis and at the cladding's outer surface, there is very little effect on the fibre's geometry and axial velocity which are determined from one–dimensional equations that employ cross–sectionally averaged temperatures.

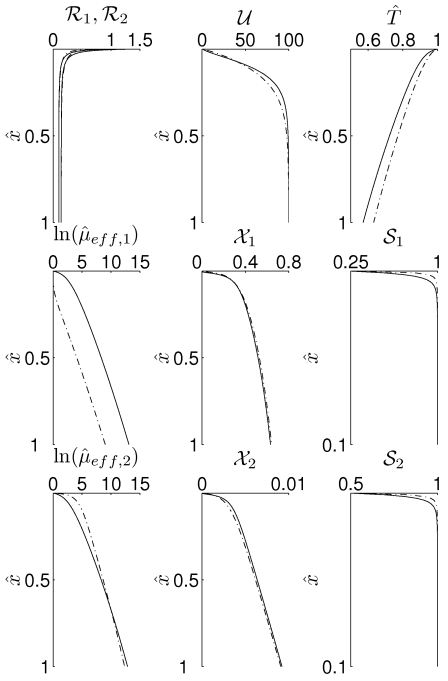

Figure 6. Comparison between one–dimensional (–) and two–dimensional models (– · –) for Case 1.

For the conditions examined here and others not presented in this paper, it has been observed that the molecular orientation parameter $\mathcal{S}$ reaches a value equal to unity very close to the section of maximun swell, i.e., $\hat{x} = 0$, and may decrease slightly after that if the source term in the equation for this parameter which depends on the velocity gradient is smaller than the Maier–Saupe potential associated with the relaxation of the molecular chains. It must be noted that, for $\Delta_T = \Delta_{S1} = \Delta_{S2} = 0$, i.e., uniform distribution of the temperature and molecular orientation parameter at the maximun swell section, there are few differences between the degrees of crystallization predicted by the 1D and 2D models because the temperature at the swelling section is assumed to be uniform.

CONCLUSIONS

A single–phase two–dimensional model of the spinning of semi–crystalline compound fibres that employs a Newtonian

rheology modified by the degrees of crystallization and molecular orientation and temperature through an effective dynamic viscosity, and accounts for the molecular orientation of the liquid crystalline polymer through an orientation tensor that depends on the velocity field, has been proposed. For slender fibres and very low Biot numbers, an asymptotic analysis yields one–dimensional equations for the leading–order axial velocity, temperature, orientation parameter and degree of crystallization provided that the molecular orientation tensor is diagonal at leading order in the slenderness ratio. For higher Biot numbers or when the orientation tensor is not diagonal at leading order, the two-dimensional model was solved numerically, and its results indicate that substantial temperature non–uniformities in the radial direction exist even at moderately low Biot numbers. These non–uniformities affect the degree of crystallization and may have great effects on the mechanical, electrical, etc., properties of compound fibres. For very slender fibres and small Biot numbers, good agreement between the leading–order one–dimensional model and the two–dimensional one has been observed. It was found that the crystallization of the compound fibre was mostly affected by thermal effects rather than by flow–induced ones for the conditions considered here.

ACKNOWLEDGMENT

The research reported in this paper was supported by Project FIS2009-12894 and FPU grant reference AP2006-02242 from the Ministerio de Ciencia e Innovación of Spain.

NOMENCLATURE

a_2 Constant of the linearized crystal growth rate $[\cdot]$
c Number of polymeric units per unit volume $[1/m^3]$
C Specific heat $[J/kgK]$
D Pre–exponential factor (linear approximation) $[Ns/m^2]$
$\mathbf{f}^m$ Body force per unit mass $[N/kg]$
g Gravitational acceleration $[m/s^2]$
h Film heat transfer coefficient $[W/Km^2]$
H Activation temperature (linear approximation) $[1/K]$
k Thermal conductivity $[W/Km]$
k_A Linearized crystal growth rate $[\cdot]$
$k_A(0)$ Amorphous growth rate $[\cdot]$
k_B Boltzmann constant $[1.3806503 \cdot 10^{-23}\ m^2 kg/s^2 K]$
L Characteristic length in the axial direction $[m]$
n Crystallization viscosity index $[\cdot]$
N Dimensionless measure of c $[\cdot]$
p Pressure $[N/m^2]$
Q Nondimensional volumetric flow rate $[\cdot]$
r Radial coordinate $[m]$
R Jet's radius $[m]$
$\mathcal{R}$ Nondimensional jet's radius $[\cdot]$
$\mathcal{S}$ Molecular orientation parameter $[\cdot]$
$\mathbf{S}$ Molecular orientation tensor $[\cdot]$
t Time $[s]$
T Temperature $[K]$
$\hat{T}$ Nondimensional temperature $[\cdot]$
T_∞ Temperature of the gases that surround the fibre $[K]$
$\mathbf{u}$ Molecular orientation vector $[\cdot]$
$\mathcal{U}$ Nondimensional axial velocity $[\cdot]$
$\mathbf{v}$ Velocity vector $[m/s]$
x Axial coordinate $[m]$
$\mathcal{X}$ Degree of crystallinity $[\cdot]$
$\mathcal{X}_\infty$ Ultimate degree of crystallinity $[\cdot]$

α Relation between kinetic energy and internal energy $[\cdot]$
β Crystallization viscosity rate $[\cdot]$
ε Slenderness ratio $[\cdot]$
η Mapping of the nondimensional axial coordinate $[\cdot]$
θ Azimuthal coordinate $[\cdot]$
λ Relaxation time $[s]$
λ_0 Relaxation time at melting temperature $[s]$
μ Dynamic viscosity $[N/m^2 s]$
ξ Mapping of the nondimensional radial coordinate $[\cdot]$
ρ Density $[kg/m^3]$
σ Surface tension $[N/m]$
τ Stress tensor $[N/m^2]$
ϕ Dimensionless parameter related to the friction tensor $[\cdot]$
ω Activation temperature for the relaxation time $[1/K]$

$_0$ Reference values
$_{eff}$ Effective
$_m$ Melting conditions

REFERENCES

[1] C.-C. Ji, J.-C. Yang and W.-S. Lee Mechanics of Steady Flow in Coextrusion Fiber Spinning, *Polym. Eng. Sci.*, vol. 36, pp. 1399-1409, 1996.
[2] W.-S. Lee and C.-W. Park, Stability of a Bicomponent Fiber Spinning Flow, *ASME J. Appl. Mech.*, vol. 62, pp. 511-516, 1995.
[3] S.K. Naboulsi and S.E. Bechtel, Bicomponent Newtonian Fibers, *Phys. Fluids*, vol. 11, pp. 807-820, 1999.
[4] J.I. Ramos, Asymptotic Analysis of Compound Liquid Jets at Low Reynolds Numbers, *Appl. Math. Comput.*, vol. 100, pp. 223-240, 1999.
[5] J.I. Ramos, Compound Liquid Jets at Low Reynolds Numbers, *Polymer*, vol. 43, pp. 2889-2896, 2002.
[6] K. Kikutani, J. Radhakrishnan, S. Arikawa, A. Takaku, N. Okui, X. Jin, F. Niwa and Y. Kudo, High–speed Melt Spinning of Bicomponent Fibers: Mechanism of Fiber Structure Development in Poly(ethylene terephthalate)/Polypropylene System, *J. Appl. Polym. Sci.*, vol. 62, pp. 1913-1924, 1996.
[7] J.I. Ramos, Modelling of Liquid Crystalline Compound Fibres, *Polymer*, vol. 46, pp. 12612-12625, 2005.
[8] M. Avrami, Kinetics of phase change. III. Granulation, Phase change, and Microstructure, *J. Chem. Phys.*, vol. 9, pp. 177-184, 1941.
[9] A.N. Kolmogorov, On the Statistical Theory of the Crystallization of Metals, *Bulletion of the Academy of Sciences of the USSR, Mathematical Series*, vol. 1, pp. 355-359, 1937.
[10] A. Ziabicki, *Fundamentals of Fibre Formation*, John Wiley & Sons, New York, 1976.
[11] A. Ziabicki and H. Kawai, *High Speed Fiber Spinning*, John Wiley & Sons, New York, 1985.
[12] A. Ziabicki, A. Jarecki and A. Wasiak, Dynamic Modelling of Melt Spinning, *Comp. and Theo. Polymer Sci.*, vol. 8, pp. 143-157, 1988.
[13] S. Kase and T. Matsuo, Studies of Melt Spinning. I. Fundamental Equations on the Dynamics of Melt Spinning, *J. Polymer Sci. A*, vol. 3, pp. 2541-2554, 1965.